Kinetic Characterization of the Polymerase and Exonuclease Activities of the Gene 43 Protein of Bacteriophage T4†

Todd L. Capson, James A. Peliska, Barbara Fenn Kaboord, Michelle West Frey, Chris Lively, Michael Dahlberg, and Stephen J. Benkovic*

Department of Chemistry, 152 Davey Laboratory, The Pennsylvania State University, University Park, Pennsylvania 16802

Received June 5, 1992; Revised Manuscript Received August 24, 1992

ABSTRACT: The DNA polymerase from the bacteriophage T4 is part of a multienzyme complex required for the synthesis of DNA. As a first step in understanding the contributions of individual proteins to the dynamic properties of the complex, e.g., turnover, processivity, and fidelity of replication, the minimal kinetic schemes for the polymerase and exonuclease activities of the gene 43 protein have been determined by pre-steady-state kinetic methods and fit by computer simulation. A DNA primer/template (13/20-mer) was used as substrate; duplexes that contained more single-strand DNA resulted in nonproductive binding of the polymerase. The reaction sequence features an ordered addition of 13/20-mer followed by dATP to the T4 enzyme (dissociation constants of 70 nM and 20 μM) followed by rapid conversion (400 s^{-1}) of the T4·13/20-mer·dATP complex to the T4·14/20-mer·PP_i product species. A slow step (2 s^{-1}) following PP_i release limits a single turnover, although this step is bypassed in multiple incorporations (13/20-mer → 17/20-mer) which occur at rates >400 s^{-1}. Competition between correct versus incorrect nucleotides relative to the template strand indicates that the dissociation constants for the incorrect nucleotides are at millimolar values, thus providing evidence that the T4 polymerase, like the T7 but unlike the Klenow fragment polymerases, discriminates by factors $>10^3$ against misincorporation in the nucleotide binding step. The exonuclease activity of the T4 enzyme requires an activation step, i.e., T4·DNA → T4·(DNA)*, whose rate constants reflect whether the 3′-terminus of the primer is matched or mismatched; for matched 13/20-mer the constant is 1 s^{-1}, and for mismatched 13T/20-mer, 5 s^{-1}. Evidence is presented from crossover experiments that this step may represent a melting of the terminus of the duplex, which is followed by rapid exonucleolytic cleavage (100 s^{-1}). In the presence of the correct dNTP, primer extension is the rate-limiting step rather than a step involving travel of the duplex between separated exonuclease and polymerase sites. Since the rate constant for 13/20-mer or 13T/20-mer dissociation from the enzyme is 6 or 8 s^{-1} and competes with that for activation, the exonucleolytic editing by the enzyme alone in a single pass is somewhat inefficient (5 s^{-1}/(8 s^{-1} + 5 s^{-1})), ca. 40%. Consequently, a major role for the accessory proteins may be to slow the rate of enzyme·substrate dissociation, thereby increasing overall fidelity and processivity.

Bacteriophage T4 DNA synthesis is catalyzed by a phage-encoded multienzyme complex (Nossal & Alberts, 1983; Alberts, 1987). Gene 43 of the T4 genome encodes the polymerase responsible for 5′–3′ DNA synthesis and 3′–5′ exonuclease activities (Goulian et al., 1968; Hershfield & Nossal, 1972; Huang & Lehman, 1972). The polymerase and exonuclease activities are enhanced by accessory proteins consisting of the products of genes 44, 62, and 45 (Mace & Alberts, 1984b; Bedinger & Alberts, 1983; Venkatesan & Nossal, 1982). These components, along with the gene 32 single-stranded DNA binding protein, form a complex capable of performing highly accurate, processive leading strand DNA synthesis.

The T4 polymerase system is an attractive target for detailed kinetic analysis for several reasons. First, a T4 replication fork can be reconstructed from purified components that catalyze leading and lagging strand synthesis at in vivo rates and accuracies. Second, there are strong similarities between the T4 and eukaryotic polymerases at the sequence level (Ito & Braithwaite, 1991). Third, DNA synthesis by the bacteriophage T4 and the eukaryotic polymerase δ complexes appears to have similar features (Tsurimoto & Stillman, 1990, 1991; Weinberg et al., 1990; Lee et al., 1991). Recently, it also has been shown that monoclonal antibodies can specifically react with both calf thymus DNA dependent adenosinetriphosphatase A and the gene 44 protein from the bacteriophage T4 DNA dependent ATPase (Mesner et al., 1991). Together these reports provide strong evidence for the similarities between the T4 and eukaryotic replication complexes, making the T4 polymerase complex a useful system to model DNA synthesis in higher organisms.

Before the role of these accessory proteins in replicative fidelity and processivity can be quantitatively assessed, a detailed kinetic mechanism by which DNA is synthesized by the T4 DNA polymerase alone must be constructed. Previous pre-steady-state kinetic studies on the Klenow fragment of *E. coli* Pol I[1] (Eger et al., 1991; Dahlberg & Benkovic, 1991; Kuchta et al., 1987, 1988) and the T7 DNA polymerase (Patel et al., 1991; Wong et al., 1991; Donlin et al., 1991) have been successful in determining the kinetic and thermodynamic factors contributing to the accurate and processive synthesis of DNA. While the steady-state kinetics of T4 DNA polymerase has been the subject of numerous studies detailing polymerization (Mace & Alberts, 1984a,b; Fairfield et al.,

† Supported by grants from the National Institutes of Health (GM13306) and the National Foundation for Cancer Research. T.L.C. and J.A.P. were recipients of National Research Fellowships.

* Address all correspondence to this author.

[1] Abbreviations: TBE, Tris·HCl/borate/EDTA; EDTA, ethylenediaminetetracetate, sodium salt; Pol I, *E. coli* DNA polymerase I; T_4·DNA, T_4 DNA polymerase–DNA complex; dNTP, deoxynucleotide triphosphate; PP_i, inorganic pyrophosphate; TLC, thin-layer chromatography; PEI cellulose, polyethyleneimine cellulose.

0006-2960/92/0431-10984$03.00/0

1983) and the fidelity of DNA synthesis (Kunkel, 1988; Reha-Krantz, 1988; Sinha, 1987; Kunkel et al., 1984; Ripley et al., 1983; Hibner & Alberts, 1980; Bessman & Reha-Krantz, 1977; Gillin & Nossal, 1976) due, in part, to the vigorous 3′–5′ exonuclease activity (Brutlag & Kornberg, 1972; Sinha, 1987; Gillin & Nossal, 1976; Muzcyzka et al., 1972), no detailed mechanistic scheme exists.

In this report the steady-state and pre-steady-state kinetics of T4 DNA polymerase are described in terms of the rates for single and multiple base incorporation as well as exonuclease excision. These results define the intrinsic properties of the gene 43 protein and will serve as a basis for understanding the role of the accessory proteins in the T4 replication complex.

EXPERIMENTAL PROCEDURES

Materials. New England Nuclear supplied [α-^{32}P]dATP, [γ-^{32}P]ATP, and (S_P)-[^{35}S]dATPαS. All unlabeled dNTPs were from Pharmacia (ultrapure). Dr. Jin Tann Chen synthesized the nonradioactive (S_P)-dATPαS. The T4 polymerase was expressed from either the plasmid pTL43W or pPS701, generous gifts from Drs. W. H. Konigsberg and N. Nossal (Lin et al., 1987), and purified as described by Rush and Konigsberg (1989). The Klenow fragment was a gift of Drs. Bryan Eger and Carlos Catalano. Polynucleotide kinase was from U.S. Biochemicals. DNA oligomers were synthesized on an Applied Biosystems 380A DNA synthesizer. Each single-stranded oligomer was purified by denaturing 20% polyacrylamide gel electrophoresis. DNA was eluted from the gel pieces with an Elutrap (Schleicher & Schuell) in TBE buffer (Maniatis et al., 1982), desalted (Sep-Pak, Waters Associates), and resuspended in distilled, deionized water. Complementary oligomers were annealed at room temperatures in distilled, deionized water, concentrated to dryness on a Speed-Vac (Savant), and resuspended in 40% aqueous glycerol/TBE. Duplex DNA (30 nmol) was separated from single-stranded DNA on a 3-mm nondenaturing (no urea) 20% acrylamide gel, visualized, and extracted as described for the single strands. Duplexes were quantitated as described by Kuchta et al. (1987). Duplexes were 5′-[^{32}P]-end-labeled as previously described (Mizrahi et al., 1986) except that conditions for end-labeling blunt-end duplexes were employed (Maniatis et al., 1982).

Methods. All rapid-quench experiments were performed at 20 °C on the instrument described by Johnson (1986). The assay buffer used in all kinetic studies unless otherwise indicated consisted of Tris·HCl (pH 8.8, 67 mM), β-mercaptoethanol (10 mM), and NaCl (60 mM). In the preincubation solution, EDTA (0.1 mM) was added to inhibit the exonuclease activity. Reactions were quenched into EDTA (0.5 M, pH 7.4) and diluted 1:1 with sequencing gel load buffer (Maniatis et al., 1982). Polymerization of hydrolysis reactions were monitored by analysis of the products on 16 or 20% sequencing gels as described by Mizrahi et al. (1986). All concentrations listed are final solution concentrations.

Determination of the Equilibrium Dissociation Constant, K_D, for the 13/20-mer. T4 polymerase (75 nM) was preincubated with 13/20-mer (12.5–200 nM) in assay buffer and 0.1 mM EDTA. The polymerase:13/20-mer complex was then mixed with dATP (10 μM) and $MgCl_2$ (7 mM). The reactions were quenched at variable times (3–300 ms) with EDTA (0.5 M) and the products analyzed as described above.

Methods for Measuring T4·DNA Dissociation Rate Constants. A. Trapping of Free Enzyme. The 13/20-mer duplex (100 nM) and T4 polymerase (0.5 μM) were preincubated in one syringe, and then mixed with an equal volume of heparin (0.5 mg/mL). The mixture was allowed to incubate for times ranging from 5 ms to 20 s, and any remaining T4·DNA complex chased to product by the addition of $MgCl_2$ (10 mM) and dATP (100 μM) with a constant reaction time of 50 ms. Reactions were quenched with 50 μL of EDTA (0.5 M). The production of 14/20-mer followed a single exponential decay from which the observed dissociation rate constant was determined. In order to evaluate the effect of the heparin trap concentration on the observed off-rate constant (k_{off}), the experiment was done at various concentrations of heparin (0.5–2.5 mg/mL). The observed k_{off} was plotted as a function of heparin concentration, and the resulting straight line was extrapolated to a zero heparin level, providing a value of 8 ± 0.7 s^{-1} for the dissociation of 13/20-mer. An identical set of conditions, except for the replacement of heparin with single-stranded calf thymus DNA (0.75, 0.9, 1 mg/mL), was used to measure k_{off} for the dissociation of the T4 pol·14/20-mer complex. k_{off} did not vary with the calf thymus DNA concentration and provided a value of 6 ± 1 s^{-1}.

B. Isotope Dilution. The [5′-^{32}P]-end-labeled 13/20-mer duplex (100 nM) was preincubated with an excess of a T4 exonuclease deficient enzyme (0.5 μM) (M. W. Frey, unpublished results) in one syringe and mixed with an equal volume of cold unlabeled 13/20-mer (0.5 μM). The mixture was allowed to react for varying amounts of time (5 ms to 20 s) and chased with $MgCl_2$ (10 mM) and dATP (100 μM) as described above. Reactions were quenched at 50 ms with EDTA (0.5 M). Labeled 14/20-mer production followed a single exponential decay, which was computer corrected for incomplete dilution. k_{off} was calculated to be 6 ± 1 s^{-1} in close agreement with values obtained from the above trapping experiments.

Determination of the Equilibrium Dissociation Constant, K_D, for dATP. T4 polymerase (1.4 μM) was incubated with 13/20-mer (0.25 μM) in assay buffer containing EDTA (0.1 mM) and mixed with dATP (2–40 μM) containing $MgCl_2$ (7 mM) in assay buffer. The reactions were quenched with EDTA (0.5 M) at variable times (3–500 ms), and the products were analyzed as described above.

Elemental Effects on the Polymerization Reaction. A solution of the 13/20-mer (300 nM) and T4 polymerase (100 nM) in EDTA (0.1 mM) was mixed with either [α-^{32}P]dATP (10 μM) or (S_P)-dATPαS (10 μM) in assay buffer and $MgCl_2$ (7 mM). The reactions were quenched with EDTA (0.5 M), and the products were analyzed as described above. The data were fit to a single exponential rate followed by a steady-state rate.

Competition Experiments. T4 polymerase (1 μM) was preincubated with 13/20-mer (0.25 μM) and EDTA (0.1 mM) in assay buffer. The polymerization reaction was initiated upon the addition of $MgCl_2$, dATP (20 μM, correct nucleotide), and an increasing concentration of dCTP (0–5 mM, incorrect nucleotide). The concentration of $MgCl_2$ was adjusted to compensate for the concentration of incorrect nucleotide in each assay. Reactions were quenched with EDTA (0.5 M) at variable times (3–150 ms). Products were analyzed as described above.

Pyrophosphorolysis. For pyrophosphorolysis experiments, the 13/20-mer was elongated to the [3′-^{32}P]14/20-mer as described earlier (Dahlberg & Benkovic, 1991). In order to remove the Klenow fragment, the reaction was stopped with 100 μL of 1:1 phenol/chloroform, and the aqueous phase was placed on a Bio-spin column (Bio-Rad) as described by the manufacturer. The concentration of the [3′-^{32}P]14/20-mer was determined by filter binding assays (Kuchta et al., 1987).

T4 polymerase (0.5 μM) was incubated with [3′-^{32}P]14/20-mer (0.1 μM), EDTA (0.1 mM), and PP_i (2 mM) in assay buffer. The reaction was initiated with the addition of $MgCl_2$ (9 mM) and dATP (50 μM) and terminated at 0.003–2 s with EDTA (0.2 M). The formation of [^{32}P]dATP was quantitated by TLC (PEI cellulose, EM Scientific) (Kuchta et al., 1987).

Multiple Turnover Experiments. T4 polymerase (1 μM) was preincubated with 13/20-mer (0.25 μM) in assay buffer containing EDTA (0.1 mM). Polymerization was initiated by the addition of $MgCl_2$ (7 mM) and 20 μM each of dATP and dGTP. Reactions were quenched at variable times (0–30 ms) in EDTA (0.5 M). The extension products (*n* through *n* + 4) were analyzed as described above.

Determination of Exonuclease Activity on 13/20-mer and 13T/20-mer. For reactions performed with excess DNA over enzyme, a solution of 13/20-mer or 13T/20-mer (0.5 μM) and T4 polymerase (0.1 μM) in EDTA (0.1 mM) was mixed with $MgCl_2$ (5 mM) in assay buffer. The reactions were quenched with EDTA (0.5 M), and the products were analyzed as described above. For reactions with excess enzyme over DNA, the same procedure was performed except the concentrations of 13/20-mer or 13T/20-mer and T4 polymerase were 0.1 and 0.5 μM, respectively. Alternatively, a solution of T4 polymerase (0.5 μM) was mixed with a second solution of 13T/20-mer (0.5 μM) in assay buffer including $MgCl_2$ (5 mM). The reactions were quenched and analyzed as described above.

Determination of Exonuclease Activity on 25–6T Primer. A solution of T4 DNA polymerase (0.5 μM) was mixed with 25–6T-mer single-stranded DNA (0.1 μM) with $MgCl_2$ (7 mM) in assay buffer. The products were analyzed as described above.

Method for Measuring Duplex Crossover between Exonuclease and Polymerase Sites. The rate at which the duplex DNA is transferred from the exonuclease to the polymerase sites was measured by monitoring the conversion of 13T/20-mer to 14/20-mer. T4 DNA polymerase (500 nM) and 13T/20-mer (100 nM) were preincubated and then mixed with $MgCl_2$ (10 mM) and [α-^{32}P]dATP (80 μM, 2500 cpm/pmol). A second reaction was performed in which single-stranded calf thymus DNA (1 mg/mL) was included in the Mg^{+2}/dATP solution to trap free polymerase. Reactions were terminated at varying times by quenching into EDTA (0.25 M). Aliquots of each time point were spotted in triplicates onto DE81 paper. Filters were washed as described in Kuchta et al. (1987). The binding efficiency of duplex DNA to DE81 was determined by spotting known quantities of ^{32}P-labeled 13T/20-mer and washing as indicated above.

Idling Turnover. Idling turnover was performed in the presence of 13/20-mer DNA (1 μM), T4 DNA polymerase (0.04 μM), $MgCl_2$ (10 mM), and [α-^{32}P]dATP (288 μM, 270 cpm/pmol) in assay buffer (pH 8.8). At reaction times up to 40 min, samples (5 μL) were withdrawn from the reaction mixture (100 μL total) and quenched into 10 μL of EDTA (100 mM). The quenched samples were spotted (1.5 μL) onto a PEI-cellulose F TLC plate, and the plate was developed in potassium phosphate (0.3 M, pH 7). The dATP and dAMP bands were located by autoradiography and excised, and their radioactivity was determined by scintillation counting. The concentration of dATP reacted was determined by multiplying the fraction converted to dAMP by the calculated initial concentration of dATP.

Data Analysis. The nonlinear regression analysis of the rate profiles was performed with either the program RS1 (BBN Software Products Corporation) run on a mini-VAX or with the program SF 17 MV Kinetic Software Package (Applied Photo-Physics Limited) on an Archimedes 310 computer. The simulations of the kinetic data were done with the program KINSIM (Barshop et al., 1983) as modified by Anderson et al. (1988).

```
13/20mer      5'TCGCAGCCGTCCA
              3'AGCGTCGGCAGGTTCCCAAA

13T/20mer     5'TCGCAGCCGTCCAT
              3'AGCGTCGGCAGGTTCCCAAA

12/36mer      5'GCCTCGCAGCCG
              3'CGGAGCGTCGGCAGGTTGGTTGAGTAGGTCTTGTTT

25/36mer      5'GCCTCGCAGCCGTCCAACCAACTCA
              3'CGGAGCGTCGGCAGGTTGGTTGAGTAGGTCTTGTTT
```

FIGURE 1: DNA substrates used to study the T4 polymerase.

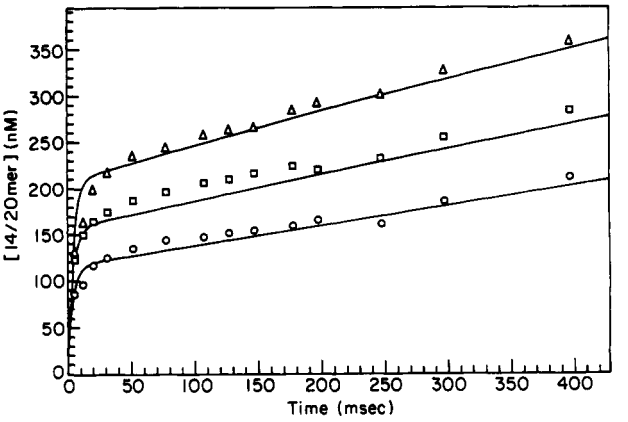

FIGURE 2: Biphasic kinetic behavior in the polymerization of 13/20-mer by T4 polymerase. Rapid-quench experiments were performed by mixing T4 polymerase (117 nM, ○; 175 nM, □; 234 nM, △) and [5′-^{32}P]-labeled DNA (800 nM) in 0.1 mM EDTA at 20 °C in assay buffer (pH 8.8) with a solution of dATP (30 μM) in assay buffer and $MgCl_2$ (7 mM). Reactions were quenched with 0.5 M EDTA (pH 7), and the products were analyzed as described in the Experimental Procedures. The solid curves were computer simulated from Scheme I.

RESULTS

Comparison of Different DNA Substrates for the Polymerization Reaction. Due to the rapid rates of the polymerization and the exonuclease activities of the T4 DNA polymerase, all of the experiments were conducted with a rapid-quench instrument. This allowed us to study the pre-steady-state kinetics of the polymerase and exonuclease reactions. Unless stated otherwise, all concentrations of reagents are final, i.e., after mixing of the components by the rapid-quench instrument. The DNA substrates used for this study are shown in Figure 1. Several DNA duplexes of varying dimensions and sequence were examined in order to determine the optimal substrate for the kinetic studies. For all of the substrates described, the duplexes were purified on nondenaturing polyacrylamide gels to remove any nonhybridized DNA. Failure to purify the duplex DNA from the single-stranded DNA either eliminated or diminished the burst of polymerization. In Figure 2 are presented the results of experiments which monitored the incorporation of a single dAMP into the primer of the 13/20-mer at varying levels of polymerase. Results obtained with the 13/20-mer were identical when either EDTA (0.1–0.5 M) or HCl (0.1–0.5 M)

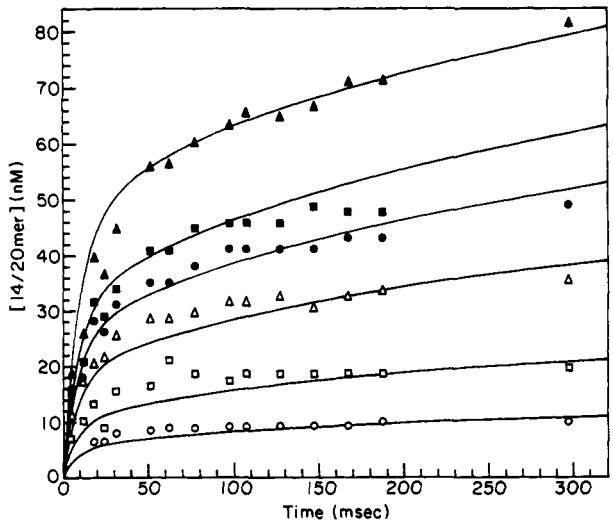

FIGURE 3: Determination of the K_d of the T4 polymerase–13/20-mer complex. Variable final concentrations of 13/20-mer (12.5 (○), 25 (□), 50 (△), 75 (●), 100 (■), and 200 nM (▲)) were incubated with T4 polymerase at 20 °C and then mixed with dATP (10 μM) and $MgCl_2$ (7 mM). The solid curves were computer simulated from Scheme I and the constants in Table I.

was used as the quench, suggesting that both solutions could stop the reaction efficiently on the rapid-quench time scale. For the 13/20-mer and the 25/36-mer, the kinetics showed a rapid burst of polymerization followed by a slower phase. The burst amplitude observed with the 25/36-mer was approximately one-half that of the 13/20-mer at the same level of enzyme, suggesting that there is one-half as much polymerase productively complexed at the primer terminus on the 25/36-mer as on the 13/20-mer (data not shown). We also examined a 12/36-duplex with the same template as the 25/36-mer, but with a primer that was 12 bases long (Figure 1). There was a slow steady-state rate of polymerization but no burst of incorporation (data not shown), implying that most of the polymerase was nonproductively complexed on the single-stranded portion of the template. On the basis of the preceding data, the 13/20-mer was chosen as the primary substrate used in determining the minimal kinetic mechanism for T4 polymerase. Protein–DNA cross-linking experiments previously showed that the polymerase interacts strongly with 5–7 bases of the duplex DNA at the primer/template terminus (Capson et al., 1991); thus, the T4 polymerase should have adequate protein contacts with the 13/20-mer.

Equilibrium Dissociation Constant of the T4·13/20-mer Complex. To measure the K_D of the 13/20-mer, the polymerization reaction was monitored with a constant concentration of T4 polymerase (75 nM) and variable amounts of 13/20-mer (12.5–200 nM). The observed pre-steady-state burst of single nucleotide incorporation is consistent with rapid template/primer elongation from an active T4·13/20-mer complex, allowing the determination of the active site concentration of the enzyme in the solution as well as the dissociation constant for the complex. The polymerase and DNA were incubated at 20 °C, mixed with a solution of dATP and $MgCl_2$, and quenched at variable times. The products were examined on DNA sequencing gels as described in the Experimental Procedures. The solid curves in Figure 3 were generated with the kinetic sequence shown in Scheme I. As the DNA concentration was increased from 12.5 to 200 nM, the amplitude of the burst increased. The slow phase of the biphasic polymerization time course increased as the DNA concentration exceeded that of the enzyme. This behavior is consistent with a slow step following the chemical step of

Scheme I

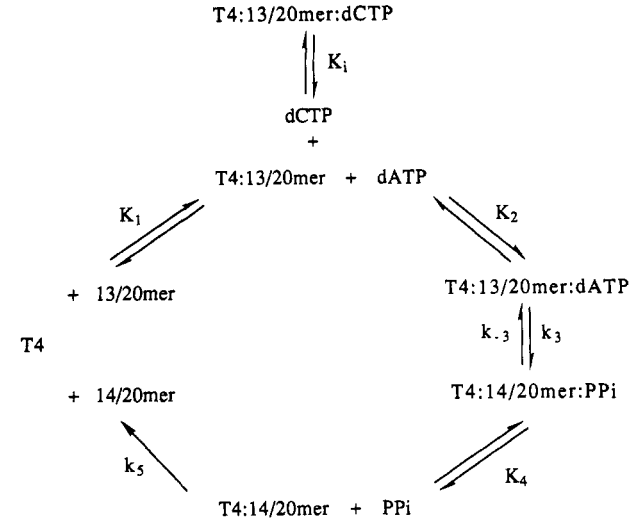

polymerization of 1–2 s^{-1} that, however, is not simply the rate constant for dissociation of T4·14/20-mer (vide infra). Extrapolation of the data from 50 to 200 ms to the product intercept on the ordinate provides the concentration of the T4·13/20-mer formed in the initial incubation and then trapped by dATP addition. The burst amplitudes were fit to the quadratic equation [T4·13/20-mer] = $0.5(K_D + [T4] + [13/20\text{-mer}] - 0.25(K_D) + [T4] + [13/20\text{-mer}])^2 - [T4\cdot13/20\text{-mer}]^{1/2}$ to provide K_D = 70 ± 7 nM. From the burst amplitude in the presence of excess DNA and the K_D of 70 nM, we calculated the concentration of active enzyme to be 35 μM, in good agreement with a value of 42 μM determined from the extinction coefficient of 125 880 M^{-1} cm^{-1} (Gill & von Hippel, 1989).

Determination of the Rate Constants for Dissociation of 13- and 14/20-mers from the T4 Binary Complexes. Two methods were used to measure the rate of dissociation of DNA duplexes from the T4 polymerase. In the first, duplex DNA was preincubated with excess T4 polymerase and then mixed with an enzyme trap (heparin or calf thymus DNA) for varying incubation times followed immediately by the addition of $MgCl_2$ and dATP. The reaction solution was quenched with EDTA after a 50-ms reaction time. Extrapolation to zero trap levels provided values of 8 ± 1 and 6 ± 1 s^{-1} for the dissociation of the T4·13/20-mer and T4·14/20-mer complexes, respectively. In the second, [5′-^{32}P]13/20-mer was preincubated with excess T4 (exonuclease deficient) polymerase and then diluted with cold 13/20-mer. At various times, the remaining T4·[5′-^{32}P]13/20-mer was chased to the labeled 14/20-mer product by the addition of $MgCl_2$ and dATP, and the latter was quantitated. From the exponential reaction progress curve, a value of 6 s^{-1} was computed for the dissociation of the T4·13/20-mer complex. Given a K_D of 70 nM for the T4·13/20-mer complex, the second-order rate constant for association of the duplex with the enzyme was calculated as 8.5 × 10^7 M^{-1} s^{-1}. This is in good agreement with a value of (2.2 ± 0.2) × 10^8 M^{-1} s^{-1} obtained from a linear replot of the initial velocities for 14/20-mer formation measured as a function of 13/20-mer concentration by the addition of duplex to enzyme.

Equilibrium Dissociation Constant for dATP from T4·13/20-mer. The experiment was performed with an excess of enzyme over DNA, conditions that allowed us to more readily measure the first-order polymerization reaction without the complication of a steady-state phase. Constant amounts of enzyme and DNA were mixed with variable quantities of

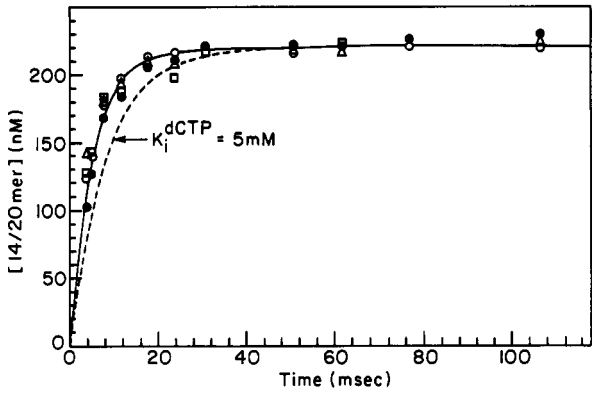

FIGURE 4: Polymerization reaction with the T4 polymerase, 13/20-mer, dATP, and increasing amounts of dCTP. A solution of the T4 polymerase, 13/20-mer, and EDTA in assay buffer was mixed with $MgCl_2$, 20 μM dATP, and dCTP at 0 (○), 250 μM (□), 1.0 mM (△), or 5.0 mM (●).

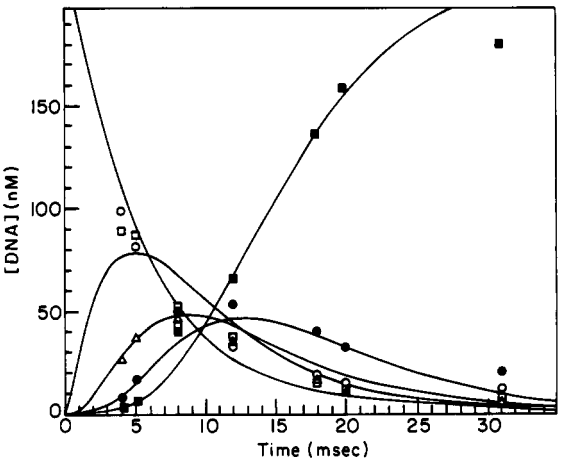

FIGURE 5: Elongation of the 13/20-mer to the 17/20-mer by T4 polymerase showing the levels of 13-(○), 14-(□), 15-(△), 16-(●), and 17-mer (■). The experimental protocol, enzyme, DNA, and nucleotide concentrations are described in the Experimental Procedures. The solid curves were generated from Scheme I, except that the observed rate of polymerization was increased from 400 s^{-1} for 14-mer production to 700 (15-mer), 1200 (16-mer), and 700 s^{-1} (17-mer). Steps for dissociation of the successive binary T4·duplex product complexes were included in the simulation.

dATP and quenched with EDTA at various times. The early portion of each polymerization time course (up to 20 ms) could be fit to a single exponential; this portion of each curve was used to determine a series of first-order rate constants (data not shown). These in turn were fit to the hyperbolic equation $k_{obsd} = k_{cat}[dATP]/([dATP] + K_D)$, yielding values of 20 ± 1 μM for K_D and 400 ± 4 s^{-1} for k_{cat}. In subsequent computer simulations of the data using Scheme I, we have assumed that the binding of dATP is at the diffusion limit.

Elemental Effects on the Polymerization Reaction. α-Phosphorothioate-substituted dNTPs have been used to infer the rate-limiting step for the polymerization reactions for the Klenow fragment and T7 polymerase (Mizrahi et al., 1985; Kuchta et al., 1987; Patel et al., 1991; Wong et al., 1991). This was based on the observation that substitution of oxygen by sulfur in phosphate triesters results in a 30–100-fold decrease in the rate of hydrolysis (Benkovic & Schray, 1971). To model reactions of phosphate diesters used in DNA and RNA synthesis more closely, Herschlag et al. (1991) examined the effect of thio substitution on the reaction of the diester, methyl 2,4-dinitrophenyl phosphate, with several different nucleophiles. Replacement of oxygen by sulfur in the diester resulted in more modest elemental effects of 4–11. Thus the intrinsic elemental effect for the chemical step of polymerization might be small. The elemental effect derived from the pre-steady-state data for the extension of the 13/20-mer to the 14/20-mer by T4 polymerase in the presence of either dATP or dATPαS at subsaturating levels is given by 120 $s^{-1}/60\ s^{-1} \approx 2$ (data not shown). Since the elemental effect is only 2-fold, the pretransient phase cannot be unambiguously attributed to either a conformational or chemical step using this criterion.

Binding of Incorrect dNTP to the T4·13/20-mer Complex. A competition experiment was designed to measure the effect of an incorrect nucleotide on the rate of correct nucleotide incorporation (Eger et al., 1991). Provided the incorrect nucleotide has a significant binding constant, the rate of correct nucleotide incorporation will decrease. We monitored the incorporation of dAMP into the 13/20-mer in the presence of varying concentrations of dCTP, up to 5 mM. As seen in Figure 4, there is a negligible effect of dCTP even when present at 5 mM, a 250-fold excess over dATP. The solid curves were computer generated from the kinetic sequence shown in Scheme I. The dashed curve in Figure 4 was generated assuming a concentration and K_i for dCTP of 5 mM; the solid curve has $K_i \approx 0$. Since the data obtained at 5 mM dCTP clearly do not fit the simulation (K_i = 5 mM), we conclude that the K_i for dCTP is >5 mM. Control experiments in which we attempted to measure the incorporation of dCTP at 5 mM in the absence of dATP showed no detectable elongation of the 13/20-mer; thus, the elongated 13/20-mer in the competition experiment must have arisen from incorporation of dAMP. Competition experiments performed with dTTP and dGTP produced similar results: under no conditions did we detect appreciable binding of the incorrect dNTPs.

Pyrophosphorolysis Experiments with the T4 Polymerase and the 14/20-mer. The reverse reaction of the polymerization is pyrophosphorolysis, i.e., excision of the 3′-terminal base by PP_i to form dNTP (Kornberg, 1980). In pyrophosphorolysis experiments with the 14/20-mer, the 3′-terminal dAMP is labeled with ^{32}P in order to measure production of radiolabeled dATP and dAMP and disappearance of the radiolabeled 14/20-mer. With increasing PP_i (2.0, 5.0, 7.5, and 10 mM), the amount of dAMP produced by the 3′–5′ exonuclease decreased while the amount of dATP produced by the pyrophosphorolysis reaction increased (data not shown). The dependence of the rate of pyrophosphorolysis on the concentration of PP_i allowed estimates of the K_D for PP_i of 10–20 mM and of rate constants of approximately 0.5 s^{-1} for the pyrophosphorolysis reaction and 1.0 s^{-1} for degradation of the 14/20-mer by the 3′–5′ exonuclease. It was necessary to include the unlabeled dATP in the assay to prevent back-incorporation of the [^{32}P]dATP generated by the pyrophosphorolysis reaction.

Multiple Incorporation. The successive incorporation of several nucleotides by T4 polymerase into the 13/20-mer should show whether the rate constant of 2 s^{-1} encountered in a single turnover can be bypassed. Any obligatory step slower than the observed rate of polymerization in the pre steady state (400 s^{-1}) will decrease the observed rate of subsequent nucleotide incorporation. The results in Figure 5 show the disappearance of the 13/20-mer and the appearance of the 14-, 15-, 16-, and 17/20-mers. The data were computer simulated using the sequence shown in Scheme I amended so that the dissociation of the T4·duplex complex competes with the addition of the next nucleotide; however, the condition of excess enzyme relative to template primer mimics a processive synthesis. We assumed that the K_D for dGTP binding to T4·duplex was equivalent to that for dATP (20 μM). A best

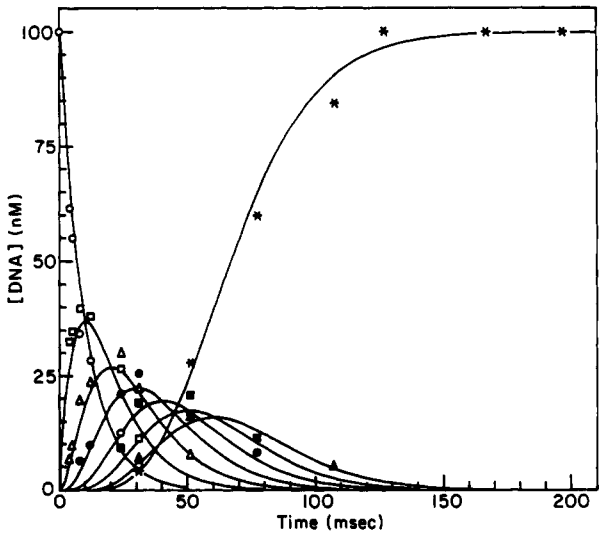

FIGURE 6: Hydrolytic cleavage by the T4 exonuclease of the 25–6T-mer single strand showing the products: 31-mer (○), 30-mer (□), 29-mer (△), 28-mer (●), 27-mer (■), 26-mer (▲), and ≤25-mer (*). The solid lines were fit to a sequential series of reactions, T4·25–6T-mer → T4·25–5T-mer → ...T4·25-mer, with the cleavage rate constant set at 100 s^{-1}.

fit simulation required adjustments of the rate constants for conversion of the central ternary substrate complex (T4·DNA·dNTP) to the product complex (T4·DNA^{n+1}·PP_i) as indicated in the figure legend. None of the incorporation steps required values <400 s^{-1}, negating the presence of a slower step in the net polymerization process between chemistry and the release of PP_i.

Exonuclease Activity. The T4 polymerase possesses an active 3′–5′ exonuclease function toward single- and double-stranded DNA. In order to establish a base-line rate for hydrolytic excision free of the effects of duplex melting, the primer strand of the 25/36-mer was tailed with six thymidine bases and used as a single-stranded substrate for the T4 exonuclease activity (Figure 6). The rate constant for hydrolytic cleavage of the individual T4·DNA complexes was the same for each excision (100 s^{-1}). If the tailed primer is annealed to the 36-mer, then the initial thymidine base is excised at 100 s^{-1}, the next three at 50 s^{-1}, and the species containing either a single mismatch or a matched 3′-terminus at <50 s^{-1} (data not shown).

To observe exonucleolytic editing on a physiologically relevant substrate (i.e., a single mismatch), the kinetics of 13T/20-mer hydrolysis was examined in detail. Incubation of the T4 polymerase with excess 13T/20-mer led to the biphasic formation of 13/20-mer characterized by a slower phase of ca. 5 s^{-1} (Figure 7a). Likewise, the production of 13/20-mer from the incubation of excess T4 polymerase with 13T/20-mer also followed a biphasic time course with a similar slower phase (Figure 7b). However, the amplitudes of the fast phases were not accurately determined in these experiments. The hydrolytic cleavage of the primer terminus matched 13/20-mer to the 12/20-mer was not biphasic over the initial 20 ms; instead, only a single exponential decay of ca. 1 s^{-1} was observed, which was abolished by the addition of a heparin trap (data not shown). Likewise, the mixing of separate solutions of T4 polymerase and 13T/20-mer under identical conditions did not produce a burst of 13/20-mer formation (data not shown).

These results suggested that either the 13/20-mer or 13T/20-mer duplex is partitioned on the enzyme in two states: one, occupied to a minor extent and visible for the 13T/20-mer, is activated for hydrolytic cleavage, and the second, populated to a major extent, is inactive for hydrolytic excision. This latter state may convert to the activated one, but at a rate slower than dissociation of the duplex from the enzyme. The forward rate constants for this conversion step are provided by the slower phases in the exonucleolytic cleavage of the 13T- and 13/20-mers. The absence of a rapid "burst" phase in experiments upon mixing the T4 polymerase and the 13T/20-mer relative to its presence when substrate and enzyme are preincubated is consistent with the absence of significant direct access from solution for binding the duplex in an activated state for exonucleolytic cleavage. This collection interpretation is formulated in Scheme II, which provides the simulations depicted in Figure 7a,b. Two types of experiments were then devised to measure the nature of the integration between the exonuclease and polymerase activities: a crossover of 13T/20-mer → 13/20-mer and nucleotide idling.

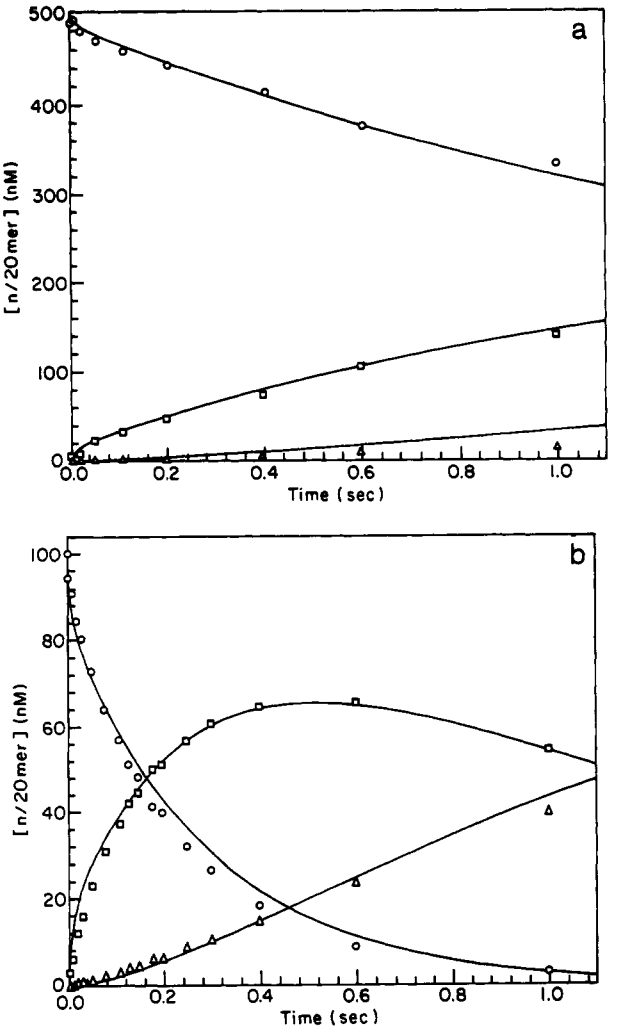

FIGURE 7: Exonucleolytic excision of 13T/20-mer (○) to form 13/20-mer (□) and 12/20-mer (△). Two experiments were conducted: in Figure 7a excess 13T/20-mer (500 nM) was preincubated with T4 polymerase (100 nM); in Figure 7b, excess T4 polymerase (500 nM) was preincubated with 13T/20-mer (100 nM). Both reactions were initiated by addition of $MgCl_2$ (7 mM) and quenched at variable times with EDTA (0.5 M). The data points were fit to Scheme II with the rate and equilibrium constants as shown.

Duplex Crossover between Exonuclease and Polymerase Activities. The steps measured by the crossover experiment are shown in Scheme III. Two studies were conducted: in the first, 13T/20-mer was incubated with T4 polymerase and mixed with [α-^{32}P]dATP and $MgCl_2$ to initiate the reaction; in the second the protocol was identical except for the presence

Scheme II

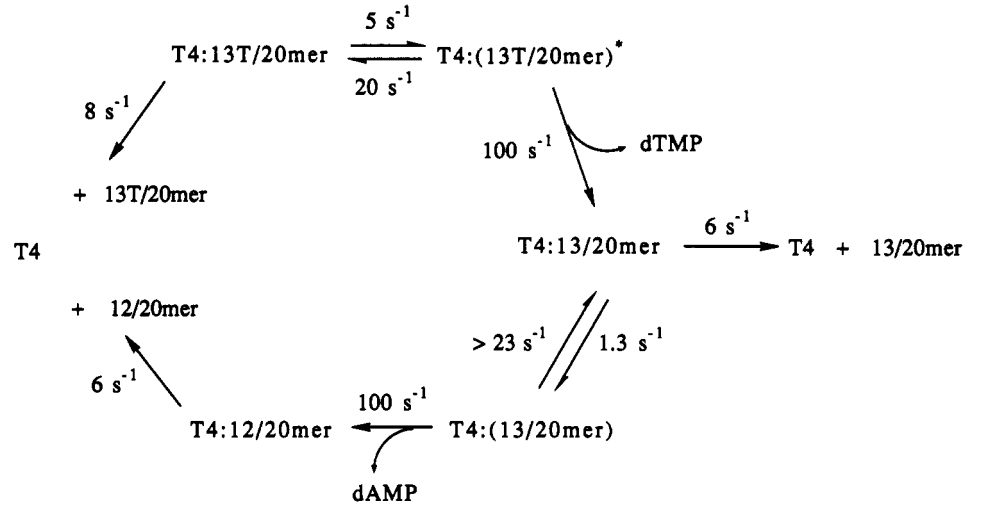

Scheme III

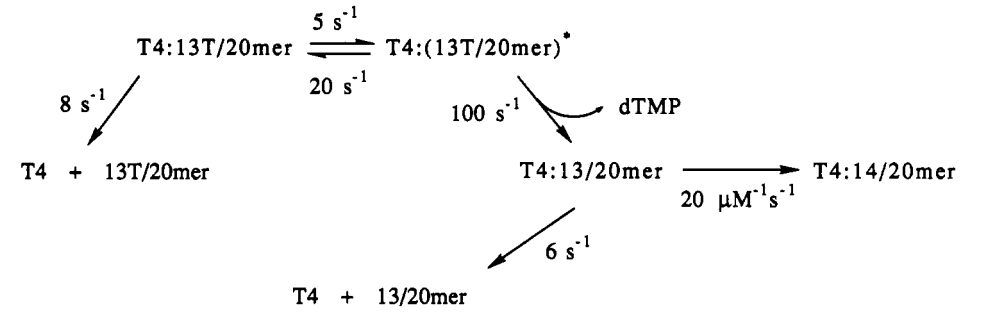

of an enzyme trap in the second solution. The results of both experiments are shown in Figure 8. In the first experiment there is a ca. 20% burst of 13/20-mer product formation at a rate of 100 s^{-1} followed by a second slower phase at ca. 5 s^{-1}. In the second, continued production of 13/20-mer is aborted by the trapping reagent after an identical initial rapid burst phase. The satisfactory fit of the simulation to the data via Scheme III, which is based on separate measurements of the exonuclease (Figures 6 and 7a,b) and the polymerase activities (Figures 2 and 3), supports the above postulate of an activation step in the exonuclease pathway and furnishes a check on those determinations. The reverse rate constant (20 s^{-1}) for the activation step is set in the case of the 13T/20-mer by the burst amplitude; for the 13/20-mer this value represents a lower limit owing to the absence of a significant burst phase. Note that, upon excision of the mismatch, the 13/20-mer·T4 complex is poised for rapid extension through the normal polymerization sequence.

Idling Turnover. The idling turnover cycle is shown in Scheme IV and is simply a cycle of nucleotide addition followed by excision. The rate of dAMP production is a measure of the idling turnover, 1 s^{-1}. Implementation of a computer simulation of Scheme IV with the denoted rate and equilibrium constants provides the fit to the idling data shown in Figure 9. The gel analysis of the duplex composition during idling revealed that 95% of the duplex was present as the 14/20-mer.

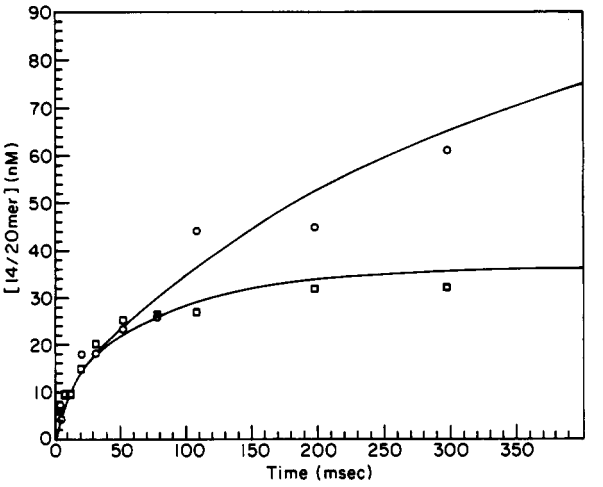

FIGURE 8: Duplex crossover between exonuclease and polymerase activities. T4 polymerase, 13T/20-mer, $MgCl_2$, and [α-^{32}P]dATP were mixed as described in the Experimental Procedures. The amount of 13T/20-mer duplex that had been correctly edited to 14/20-mer was measured in the absence (○) and in the presence (□) of a calf thymus DNA trap. The solid curves were computer simulated on the basis of the mechanism in Scheme III.

DISCUSSION

The results presented in this article have allowed us to develop minimal kinetic schemes for the polymerase (Scheme I) and exonuclease (Scheme II) activities of the T4 enzyme and their integration in editing (Scheme III) and idling (Scheme IV) processes. These schemes, constructed with the rate constants listed in Table I or in Schemes II–IV, were used to computer simulate the data for all of the figures.

Polymerization. Incorporation of a single dAMP into the 13/20-mer by the T4 polymerase follows a minimal five-step sequence with the initial productive binding of enzyme to DNA being template/primer length dependent. The results for multiple incorporation (Figure 5) reflect a modest sensitivity of the k_3 step to the identity of the dNMP; the observed variation in pre-steady-state burst amplitude implicates the single-strand length of the template as affecting productive enzyme binding. As the enzyme concentration determined

Scheme IV

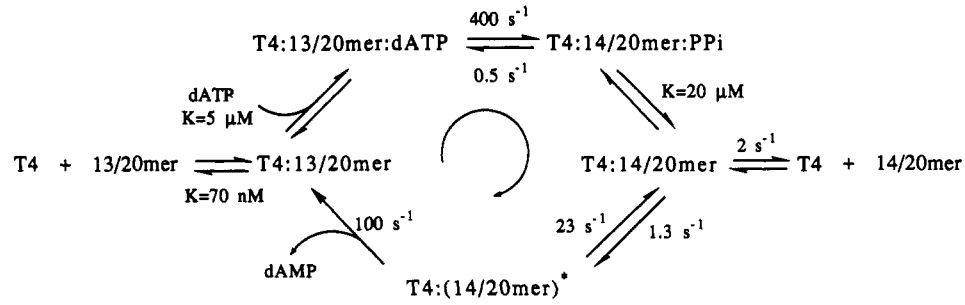

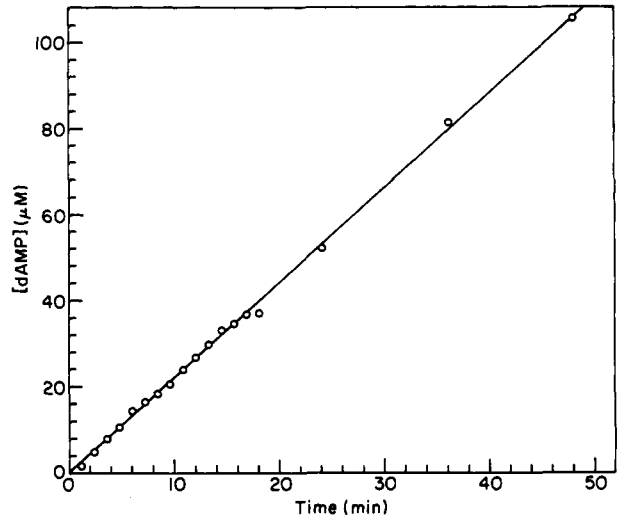

FIGURE 9: Idling turnover of dATP to dAMP by T4 DNA polymerase on 13/20-mer. The solid curve was computer simulated on the basis of the mechanism in Scheme IV.

from the burst amplitude is in good agreement with the concentration determined spectrophotometrically (Gill & von Hippel, 1989), we assume that there is one polymerase bound per 13/20-mer. The burst amplitude obtained with the 25/36-mer, however, is one-half that observed with the 13/20-mer; thus is appears that the 25/36-mer will bind polymerase unproductively. There was no detectable burst of incorporation with the 12/36-mer substrate, indicating that the polymerase was nonproductively bound on the increased single-stranded portion of the template consistent with a T4 single-strand dissociation constant of <70 nM. The decreased burst amplitudes observed with the largest DNA template substrates (12/36- and 25/36-mers) suggest that the polymerase accessory proteins have a major role in facilitating the binding of polymerase to the primer terminus, thus avoiding nonproductive binding of polymerase to other portions of the DNA substrate. Other support for this concept has been obtained from protein–DNA cross-linking studies with the T4 polymerase, polymerase accessory proteins, and 32 protein (Capson et al., 1991) and footprinting experiments by Munn and Alberts (1991a,b).

The biphasic nature of the nucleotide incorporation permitted the direct titration of the T4 polymerase site with 13/20-mer and the consequent determination of the dissociation constant (K_I) for the T4·13/20-mer complex. The rate constants for dissociation of both the T4·13/20-mer and T4·14/20-mer binary complexes are identical within error, as determined by trap and dilution methods. We have used a value of 6 s^{-1} in our simulations. The rate of dissociation is much faster than that observed with either the Klenow fragment (0.06 s^{-1}) (Kuchta et al., 1987) or T7 DNA polymerase (0.2 s^{-1}) (Patel et al., 1991) from comparable duplexes. Since the T4 polymerase accessory proteins are known to enhance the processivity of DNA polymerization (Mace & Alberts, 1984b), a significant decrease in the rate of duplex dissociation would be expected when measured in the presence of these proteins.

The dissociation constant for dATP from the T4·13/20-mer·dATP complex was measured directly from the pre-steady-state transients arising from dATP titration of the T4·13/20-mer binary complex. The K_D of 20 μM is similar to the K_m of 17 μM found on the poly(dA–dT) template (Gillin & Nossal, 1976), but higher than the values of 1–2 μM found for each of the four dNTPs on salmon sperm DNA (Gillin & Nossal, 1975). The observed rate constant for single nucleotide incorporation (>400 s^{-1}) is comparable with reported rates of DNA replication with the accessory proteins of about 600 s^{-1} at 37 °C (McCarthy et al., 1976). This is consistent with the suggestion of Mace and Alberts (1984b) that the stimulatory effect of the accessory proteins is due solely to a change in the processivity of polymerization and not to an increase in the rate of the polymerization reaction per se.

Pyrophosphorolysis on the 14/20-mer product occurs at saturating pyrophosphate levels with a rate constant of ca. 0.5 s^{-1}. For now, this value as well as that for nucleotide incorporation (400 s^{-1}) is arbitrarily assigned to the chemical steps k_3 and k_{-3}. Unlike the Klenow fragment (Dahlberg & Benkovic, 1991) where the burst amplitude in a single turnover experiment at saturating DNA and dNTP levels is 80% of the expected stoichiometry, in the T4 case, the amount of turnover matches the enzyme concentration and is independent of the nature of the quench. Consequently, there is no evidence for the accumulation of ternary substrate/product complexes isolated by slower nonchemical steps. For the T7 polymerase enzyme (Patel et al., 1991), the pre-steady-state turnover rate was assigned to a conformational change preceding the chemical step. This conclusion was based on a pre-steady-state pulse/chase experiment, which provided direct evidence for the existence of two enzyme·DNA·dNTP complexes and measured their relative partitioning to extended template/primer or dissociated unchanged duplex. However, their dissection of the partitioning ratio and the evaluation of the individual rate coefficients are severely compromised by the unsupported assumption of an intrinsic phosphorothioate elemental effect of 100 (Wong et al., 1991), which was used in the analysis. The use of thio effects to establish rate-limiting steps with the Klenow fragment is further complicated by the possibility of differential binding affinities for oxo versus thio substrates (Dahlberg & Benkovic, 1991) and possible steric clash in the transition state upon substitution of oxygen with sulfur (Polesky et al., 1992). For the T4 enzyme, the presence of a nonchemical step interposed between the product complexes, T4·14/20·PP_i and T4·14/20, is not manifest during the multiple incorporation of several dNMPs to form the 17/20-mer, since there is no decrease in the rate of incorporation

Table I: Kinetic Parameters for T4 Polymerase and Exonuclease Activities

reaction	kinetic constants		
	k^+	k^-	K_D
$T4 + 13/20 \underset{k_{-1}}{\overset{k_1}{\rightleftharpoons}} T4{\cdot}13/20$	$8.5 \times 10^7\ M^{-1}\ s^{-1}$	$6\ s^{-1}$ [d]	70 nM
$T4 + 14/20 \underset{k_{-1}}{\overset{}{\rightleftharpoons}} T4{\cdot}14/20$	nD	$6\ s^{-1}$	nD
$T4{\cdot}13/20 + dATP \underset{k^{-2}}{\overset{k_2}{\rightleftharpoons}} T4{\cdot}13/20{\cdot}dATP$	$(1.0 \times 10^8\ M^{-1}\ s^{-1})$[a]	$(2000\ s^{-1})$[a]	20 μM
$T4{\cdot}13/20{\cdot}dATP \underset{k_{-3}}{\overset{k_3}{\rightleftharpoons}} T4{\cdot}14/20{\cdot}PP_i$	$(400\ s^{-1})$[b]	$(0.5\ s^{-1})$[b]	
$T4{\cdot}14/20 + PP_i \underset{k_{-4}}{\overset{k_4}{\rightleftharpoons}} T4{\cdot}14/20{\cdot}PP_i$	nD	nD	10–20 mM
$T4 + 14/20 \underset{}{\overset{k_5}{\rightleftharpoons}} T4{\cdot}14/20$	$(2\ s^{-1})$[c]	nD	

[a] Numbers in parentheses are assumed values. [b] Arbitrarily assigned. [c] Observed steady-state rate. [d] From the isotope dilution experiment.

for each subsequent dNMP. Therefore, any such step, if present, must exceed 400 s^{-1}. Although by analogy to both the Klenow fragment and T7 polymerase, conformational change steps may well flank the chemical steps (k_3 and k_{-3}) performed by the T4 enzyme; their precise evaluation is elusive.

The final step in the polymerization cycle gives rise to the observed steady-state velocity, which has a k_{cat} of ca. 2 s^{-1}. Although dissociation of $E{\cdot}DNA_{n+1}$ is largely rate-limiting for the Klenow and T7 enzymes, direct measurement shows that the rate constant for 14/20-mer dissociation from the T4 enzyme is 3-fold faster than k_{cat}. Thus, it appears that the last step in the cycle is not simply product dissociation from the polymerase site. Rather, the data suggest that following chemistry the enzyme may be in an altered conformational state that possesses increased DNA affinity which, in turn, may be related to the higher affinity state achieved through its association with the accessory proteins.

The polymerization process for the T4 enzyme is further distinguished by a high degree of nucleotide triphosphate discrimination in dNTP binding to the T4·DNA complex. Experiments in which we monitored incorporation of the correct dNTP in the presence of large quantities of incorrect dNTPs (Figure 4) indicate that the T4 polymerase is extremely effective at binding the correct dNTP. Even in the presence of a 250-fold excess of an incorrect dNTP, there was no significant decrease in the observed rate of incorporation of the correct dNTP. These competition experiments imply that a significant degree of the accuracy of the T4 polymerase is due to discrimination between correct and incorrect dNTPs. Our results are consistent with those of Gillin and Nossal, who reported K_m's up to 267-fold greater for utilization of the noncomplementary dNTP compared to the complementary dNTPs (Gillin & Nossal, 1976; Topal et al., 1980). A similar result was obtained for the T7 polymerase, in which competition experiments showed that the K_i for an incorrect dNTP (dCTP) was 6–8 mM, compared to the K_D for the correct dNTP (dTTP) of 18 μM (Wong et al., 1991). Thus, results with the T4 and T7 polymerases are in contrast to those obtained with the Klenow fragment of Pol I in which the correct dNTP was bound with the same affinity as the incorrect dNTP (Eger et al., 1991). This may be a reflection of the roles that the T4 and T7 polymerases play as true replicative polymerases, whereas the *E. coli* Pol I serves as a repair enzyme.

Exonuclease Activity. The T4 enzyme exhibits an active 3′–5′ exonuclease activity toward both single-strand and duplex DNA. Hydrolysis of the single-strand substrate derived from the 25-mer (Figure 6) proceeds with the successive excision of five 3′-terminal thymidines at 100 s^{-1}/TMP without the intervention of a slower dissociation step for single-strand loss from the binary complex, in accord with a processive excision process. Annealing of this primer to the 36-mer template likewise produced a processive excision pattern with a reduction in the hydrolytic cleavage rate only after a single mismatch or a mismatched 3′-terminus was achieved. We interpret the value of 100 s^{-1} as the intrinsic cleavage rate for the exonuclease site independent of the effects of duplex melting.

At the single mismatch level, i.e., the 13T/20-mer, the kinetics of the exonuclease activity are described by Scheme II with the values of the rate constants indicated. Binding of the 13T/20-mer to the T4 enzyme provides both activated, T4·(13T/20-mer)*, and unactivated, T4·13T/20-mer, binary complexes in approximately a 1:5 ratio with the former poised for rapid excision of the terminal TMP. The relatively slow conversion of T4·13T/20-mer to the active complex (5 s^{-1}) versus the rate of dissociation of the duplex from the enzyme (8 s^{-1}) leads to the termination of the hydrolysis after partial reaction in the presence of trapping reagents. The correctly base-paired T4·13/20-mer product complex similarly prefers to dissociate (6 s^{-1}) relative to its conversion (1 s^{-1}) to an analogous activated complex, with the equilibrium between the T4·(13/20-mer)* and T4·13/20-mer complexes in approximately a 1:23 ratio. We will defer discussion of the nature of the activation step until further consideration of an experimental situation involving mismatch editing where both polymerase and exonuclease activities are operative.

This kinetic barrier, although not absolute, has the benefit of protecting properly base-paired 3′-termini from hydrolytic excision. Note that there is no measurable direct access to the activated, exonucleolytic complex from solution in contrast to the exonuclease site of the T7 polymerase enzyme (Donlin et al., 1991). We did not observe a burst of excised nucleotide product when a duplex containing either a single 3′-mismatch or a correctly paired terminus was mixed with the polymerase enzyme to initiate the reaction. An initial rapid phase was observed under these conditions if the DNA duplex had not been rigorously purified to remove unannealed single-strand primer. On the other hand, preincubation of the T4 enzyme with 3′-mismatched duplex before initiating the reaction by addition of Mg^{2+} led to biphasic dNMP formation. This is in contrast to the T7 polymerase where only a single slow phase associated with a rate constant of 2.3 s^{-1} (0.2 s^{-1} for a

Scheme V

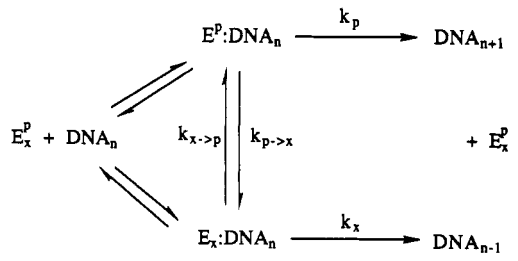

matched DNA) was observed for excision. The near identity between this value (the authors used a 26T/36-mer) and our value of 5 s^{-1} (1 s^{-1} for a matched DNA) suggests that the two enzymes share a common mechanistic activation feature.

Editing. The crossover experiment illustrated in Scheme III requires the exonucleolytic editing of a 3′-terminus TMP mismatch and its replacement by dAMP through the polymerization process. There is no nucleotide synthesis onto a mismatched 3′-terminus under our conditions (M. W. Frey, unpublished results). Carrying out the experiment in the presence of an efficient trap for free enzyme permits the evaluation of the intramolecular processes open to the enzyme, namely, the ability to switch between the polymerase and exonuclease modes without dissociation of the duplex. This switching is essential for efficient editing of the product of the polymerase reaction and, it is presumed, is more facile in a replicative complex than with the polymerase alone.

The results depicted in Scheme III indicate that a kinetic as opposed to an equilibrium partitioning model applies to the T4 enzyme. That is, the rate for interconverting the two binary T4 enzyme complexes is slower than the rate for either the hydrolytic excision or the escape of the duplex from the unactivated complex. Consequently, the net total conversion of 13T/20-mer to 14/20-mer is interrupted by the presence of trapping reagent. Nevertheless the intramolecular activation step is partially operative (5 s^{-1}/(5 s^{-1} + 8 s^{-1})) after the initial fast formation of 14/20-mer in the biphasic progress curve. The reader should note that there is no requirement for imposition of a kinetic step between formation of the T4·13/20-mer in the exonucleolytic cleavage process and the onset of the polymerization extension.

In contrast, the related response of the T7 polymerase to DNA containing a single 3′-terminal mismatch has been described in terms of bidirectional channeling between the polymerase and exonuclease sites (Donlin, 1991). These sites, in analogy with the Klenow fragment, are presumed to be spatially distinct (Ollis et al., 1985) (Scheme V). However, there is an alternate interpretation. Firstly, the values of the relevant parameters k_{p-x} and k_{x-p} are 2.3 and 714 s^{-1} for a 26T/36-mer duplex. The higher value of k_{x-p} is required for the data fit, owing to the apparent dissociation of DNA directly from the exonuclease site. However, k_{p-x} is quantitatively similar to that observed with the T4 enzyme. Secondly, experiments by Cowart et al. (1989) using a synthetic cross-linked primer/template suggest that a minimum of five bases must be available for melting before primer excision by the Klenow fragment. This observation is in accord with previously published crystallographic data on the Klenow fragment (Ollis et al., 1985). In contrast, only one to two bases are involved in the activation step for both the T4 and T7 polymerases. Although these latter data do not unambiguously reveal the spatial relationship between the two putative sites, the cross-linking experiments may indeed reveal the degree of melting of the primer strand needed for excision to occur. It would seem reasonable, therefore, to interpret the activation step in the T4 enzyme, and by analogy the k_{p-x} step for the T7 enzyme, as associated with a melting phenomenon, followed by rapid excision of the terminal 3′-base. On our time scale, there is no evidence for a kinetically significant step for primer repositioning relative to the rapid polymerization cycle. Indeed duplex crossover experiments at a higher temperature (30 °C vs 20 °C) reveal a 2-fold increase in the initial population of the activated complex and an increased rate (2.5-fold) for its formation, consistent with a melting of the duplex in this step (B. Fenn Kaboord, unpublished results).

Idling. The idling cycle, a process in which the enzyme catalyzes the addition of dATP and then excises it in the absence of the next required nucleotide triphosphate, is shown in Scheme IV. The gel analysis of the duplex composition during idling revealed that 95% of the DNA was present as the 14/20-mer. This result is again consistent with the absence of a significant direct access from solution to the activated T4·(DNA)* species for exonucleolytic cleavage. An idling mechanism consisting of direct access of the DNA duplex to the exonuclease site would give ratios of 13/20-mer to 14/20-mer approaching 1:1 since the steady-state rate of nucleotide incorporation competes with that of exonucleolytic excision (both occurring at observed rates of ca. 1 s^{-1}).

The nearly complete absence of 13/20-mer duplex during steady-state idling turnover suggests that the 14/20-mer DNA duplex partitions on the enzyme predominantly toward the unactivated state. After the 14/20-mer is activated for hydrolytic cleavage (at a rate of 1 s^{-1}), dATP is rapidly incorporated without duplex dissociation from the enzyme. This model then accounts for the large steady-state excess of 14/20-mer over 13/20-mer during idling turnover and is also consistent with the low accumulation of dNMP during multiple turnovers.

CONCLUSION

Having defined a minimal kinetic scheme for the polymerization reaction by the T4 polymerase alone, we are now in a position to further examine the roles of the T4 accessory proteins to determine where their effects are manifest in the synthesis of T4 DNA. A recent report by Tsurimoto and Stillman (1990) pointed out similarities between DNA synthesis by the phage T4 and the eukaryotic δ polymerase and its attendant accessory proteins. Thus, studies of T4 DNA replication should provide insight into DNA synthesis in higher organisms. We already can suggest that the accessory proteins do not increase the intrinsic polymerization rate but do influence the degree of productive complexation at the 3′-terminus of the primer. In addition, they are not important in nucleotide triphosphate recognition, but may act to prevent dissociation of the enzyme from a mismatched 3′-terminal primer duplex prior to the exonuclease activation step, thereby increasing exonuclease editing and improving fidelity.

REFERENCES

Alberts, B. M. (1987) *Philos. Trans. R. Soc. London B 317*, 395–420.

Anderson, K., Silorski, J. A., & Johnson, K. A. (1988) *Biochemistry 27*, 7395–7406.

Barshop, B. A., Wrenn, R. F., & Frieden, C. (1983) *Anal. Biochem. 130*, 134–145.

Bedinger, P., & Alberts, B. M. (1983) *J. Biol. Chem. 258*, 9649–9656.

Benkovic, S. J., & Schray, K. J. (1971) in *The Enzymes* Boyer, P. D., Ed.) 3rd ed., Vol. 8, pp 201–238, Academic, New York.

Bessman, M. J., & Reha-Krantz, L. J. (1977) *J. Mol. Biol. 116*, 115–123.

Brutlag, D., & Kornberg, A. (1972) *J. Biol. Chem. 247*, 241–248.
Capson, T. L., Benkovic, S. J., & Nossal, N. G. (1991) *Cell 65*, 240–258.
Dahlberg, M. E., & Benkovic, S. J. (1991) *Biochemistry 30*, 4835–4843.
Donlin, M. J., Patel, S. S., & Johnson, K. A. (1991) *Biochemistry 30*, 538–546.
Eger, B. T., Kuchta, R. D., Carroll, S. S., Benkovic, P. A., Dahlberg, M. E., Joyce, C. M., & Benkovic, S. J. (1991) *Biochemistry 30*, 1441–1448.
Fairfield, F. R., Newport, J. W., Dolejsi, M. K., & von Hippel, P. H. (1983) *J. Biomol. Struct. Dyn. 1*, 715–727.
Gill, S. C., & von Hippel, P. H. (1989) *Anal. Biochem. 182*, 319–326.
Gillin, F. D., & Nossal, N. G. (1975) *Biochem. Biophys. Res. Commun. 64*, 457–464.
Gillin, F. D., & Nossal, N. G. (1976) *J. Biol. Chem. 251*, 5225–5232.
Goulian, M., Lucas, Z. T., & Kornberg, A. (1968) *J. Biol. Chem. 243*, 627–638.
Herschlag, D., Picirilli, J. A., & Cech, T. R. (1991) *Biochemistry 30*, 4844–4854.
Hershfield, M. S., & Nossal, N. G. (1972) *J. Biol. Chem. 247*, 3393–3404.
Hibner, U., & Alberts, B. M. (1980) *Nature 285*, 300–305.
Huang, W. M., & Lehman, I. R. (1972) *J. Biol. Chem. 247*, 3139–3146.
Ito, J., & Braithwaite, D. K. (1991) *Nucleic Acids. Res. 19*, 4045–4057.
Johnson, K. A. (1986) *Methods Enzymol. 134*, 677–705.
Kornberg, A. (1980) *DNA Replication* Freeman, San Francisco.
Kuchta, R. D., Mizrahi, V. M., Benkovic, P. A., Johnson, K. A., & Benkovic, S. J. (1987) *Biochemistry 26*, 8410–8427.
Kuchta, R. D., Benkovic, P. A., & Benkovic, S. J. (1988) *Biochemistry 27*, 6716–6725.
Kunkel, T. A. (1988) *Cell 53*, 837–840.
Kunkel, T. A., Loeb, L. A., & Goodman, M. F. (1984) *J. Biol. Chem. 259*, 1539–1545.
Lee, S. H., Kwong, A. D., Pan, Z.-Q., & Hurwitz, J. (1991) *J. Biol. Chem. 266*, 594–602.
Lin, T.-C., Rush, J., Spicer, E. K., & Konigsberg, W. H. (1987) *Proc. Natl. Acad. Sci. U.S.A. 84*, 7000–7004.
Mace, D. C., & Alberts, B. M. (1984a) *J. Mol. Biol. 177*, 295–311.
Mace, D. C., & Alberts, B. M. (1984b) *J. Mol. Biol. 177*, 313–327.
Maniatis, T., Fritsch, E. F., & Sambrook, J. (1982) *Molecular Cloning*. A Laboratory Manual, Cold Spring Harbor, New York.
McCarthy, D., Minner, C., Bernstein, H., & Bernstein, C. (1976) *J. Mol. Biol. 106*, 963–981.
Mesner, L. D., Sutherlund, W. M., & Hockensmith, J. W. (1991) *Biochemistry 30*, 11490–11494.
Mizrahi, V., Henrie, R. N., Marlier, J. F., Johnson, K. A., & Benkovic, S. J. (1985) *Biochemistry 24*, 4010–4018.
Mizrahi, V., Benkovic, P. A., & Benkovic, S. J. (1986) *Proc. Natl. Acad. U.S.A. 83*, 5769–5773.
Munn, M. M., & Alberts, B. M. (1991a) *J. Biol. Chem. 266*, 20024–20033.
Munn, M. M., & Alberts, B. M. (1991b) *J. Biol. Chem. 266*, 20034–20044.
Muzyczka, N., Poland, R. L., & Bessman, M. J. (1972) *J. Biol. Chem. 247*, 7116–7122.
Nossal, N. G., & Alberts, B. M. (1983) in *Bacteriophage T4* (Mathews, C. K., Kutter, C. M., Mosig, G., & Berget, P. B., Eds.) pp 71–81, American Society for Microbiology, Washington, D.C.
Ollis, D. L., Buck, P., Hamlin, R., Xuong, N. G., & Steitz, T. A. (1985) *Nature (London) 313*, 762–766.
Patel, S. S., Wong, I., & Johnson, K. A. (1991) *Biochemistry 30*, 511–525.
Polesky, A. H., Dahlberg, M. E., Benklovic, S. J., Grindley, N. D. F., & Joyce, C. M. (1992) *J. Biol. Chem. 267*, 8417–8428.
Reha-Krantz, L. J. (1988) *J. Mol. Biol. 202*, 711–724.
Ripley, L. S., Glickman, B. W., & Shoemaker, N. B. (1983) *Mol. Gen. Genet. 189*, 113–117.
Rush, J., & Konigsberg, W. H. (1989) *Prep. Biochem. 19*, 329–340.
Sinha, N. (1987) *Proc. Natl. Acad. Sci. U.S.A. 84*, 915–919.
Topal, M. D., DiGuiseppi, S. R., & Sinha, N, K. (1980) *J. Biol. Chem. 255*, 11717–11724.
Tsurimoto, T., & Stillman, B. (1990) *Proc. Natl. Acad. U.S.A. 87*, 1023–1027.
Tsurimoto, T., & Stillman, B. (1991) *J. Biol. Chem. 266*, 1950-1960.
Venkatesan, M., & Nossal, N. G. (1982) *J. Biol. Chem. 257*, 12435–12443.
Weinberg, D. H., Collins, K. L., Simancek, P., Russo, A., Wold, M. S., Virshup, A. M., & Kelly, T. J. (1990) *Proc. Natl. Acad. Sci. U.S.A. 87*, 8692–8696.
Wong, I. W., Patel, S. S., & Johnson, K. A. (1991) *Biochemistry 30*, 526–537.